Friction torque in four contact point slewing bearings: effect of manufacturing errors and ring stiffness

Iker Heras[1], Josu Aguirrebeitia[1], Mikel Abasolo[1]
[1] Department of Mechanical Engineering, University of the Basque Country, Bilbao, Spain

ABSTRACT

This work outlines a procedure for the determination of the interferences between balls and raceways in four contact point slewing bearings due to manufacturing errors. The procedure is applied to a particular case and finite element analyses are performed for the friction torque calculation, considering different preloads. The results are used to evaluate the influence of manufacturing errors and the stiffness of the rings in the idling friction torque of the bearing.

KEYWORDS
four contact point bearing, slewing bearing, friction torque, manufacturing errors, ring stiffness

1. INTRODUCTION

Friction torque is a key parameter when designing slewing bearings. This type of bearing is used for orientation purposes in machines like tower cranes or wind turbines, where large loads are involved (Figure 1), and also in applications where high-precision operations are required, like robots, where loading conditions are less demanding. An actuation system is needed to trigger the rotation, so the friction torque must be estimated in order to dimension it.
The first step to calculate the friction torque consists on determining the load distribution among the balls. This problem was analytically solved by Zupan and Prebil [1] and Amasorrain et al. [2]; in those models the rings where assumed to be rigid. In the same line but with a different focus, Aguirrebeitia et al. [3] [4] [5] proposed a procedure for calculating the load combinations that result in static failure, considering both ball preload and the variation of the ball-raceway contact angle with the external load.
Once the normal loads in balls are known, the tangential forces are required in order to calculate the friction torque. With this aim, Leblanc et al. [6] [7] developed an analytical model which solved the ball kinematics, which was later simplified for low-speed applications by Joshi et al. [8], and then used for the formulation of the friction torque. This model, which is based on Jones equations [9], assumes full sliding in the ball-raceway contacts, so the effects of the possible stick regions in the contact are not considered. Recently, a Finite Element (FE) model was developed by Aguirrebeitia et al. [10] for the calculation of the friction torque, where those effects are taken into account.

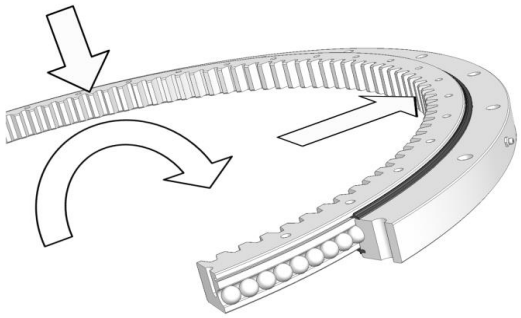

Figure 1. Loads acting on a slewing bearing

Slewing bearings are usually preloaded by introducing slightly oversized balls, avoiding thus the possible clearances due to manufacturing tolerances. The purpose of the preload is to improve the behaviour of the bearing, reducing the vibratory and runout phenomena in the assembly and increasing its stiffness [11]. However, the preload also involves an increment of the friction torque, so a balanced solution has to be found.
Manufacturing errors are also a factor to be considered. This was studied by Aithal et al. [12], who established that manufacturing tolerances affect the load distribution among the balls in this type of bearings.
Other relevant aspect that affects significantly the load distribution is the stiffness of the rings. Olave et al. [13] proposed and validated through FE calculations a procedure to obtain the load distribution in four contact point slewing bearings, considering the effect of the structure's elasticity. From the comparison with the case with rigid rings, this study proves the need for considering the stiffness of the rings for the accurate assessment of the load distribution problem.
The main objective of the present manuscript is to develop a procedure to calculate the interferences between the ball and the raceways of the bearing due to manufacturing errors. These errors are obtained for a particular case and their effect in the idling friction torque is evaluated by means of FE calculations, where both rigid and deformable rings are used in order to quantify also the influence of the stiffness of the rings. The idling friction torque is the moment required to rotate the bearing under no external loads. The idling friction torque is easily measurable and it is commonly used by bearing manufacturers as a straightforward way to adjust the preload level required for a

particular application. Along with the starting and the running torque, the idling torque is usually demanded by the customers, and thus it is a very relevant parameter.

2. INTERFERENCES CALCULATION PROCEDURE

In this section, a procedure for the determination of the interferences between the ball and the raceways due to manufacturing errors is proposed. For this purpose, an analytical model has been developed. This model needs the real shape of the raceways as input, so some experimental measurements must be taken as a first step (Figure 2a).

2.1. Measurement of the raceway geometry

To determine the real shape of a raceway, a minimum set of three points is required per each circumferential position to be considered. This way, the circumference that defines the centre and the radius of the raceway can be calculated. For a double arched ring, at least 6 points are needed per each circumferential position (see Figure 2b). To obtain the general shape of a ring, these measurements must be taken for several circumferential positions.
Since the measurements are taken for each ring separately, the relative position between them once the bearing is assembled is unknown. The analytical model described in the following subsection aims to determine this position, from which the ball-raceway interferences will be calculated.
For the measurements, a coordinate-measuring machine (CMM) was used (DEA Global Silver 12.15.10). As it is shown in Figure 2c, especial attention must be taken when measuring surfaces are neither flat nor normal to the approximation direction of the sensor probe. For the particular case to which concerns this work, the CMM was programmed to report the point R, according to Figure 2c. From the reported coordinates, it is straightforward to place the location of the centre of the probe (point O), from which the coordinates of each raceway centre can be obtained, as well as its radius.

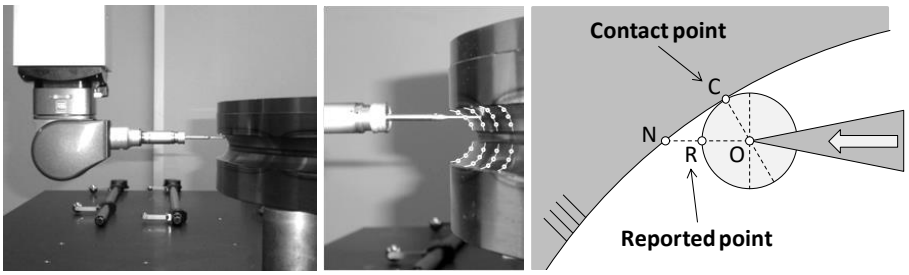

(a) (b) (c)

Figure 2. Experimental measurements: (a) coordinate-measuring machine; (b) measured points (c); graphical representation of the probe in contact with the raceway meter [14]

The results shown in this manuscript were obtained for a bearing with nominal dimensions reported in Table 1. In order to check for repeatability, the measures were taken twice for each ring. It was also checked that the different measures from the same raceway were coherent between them.

Bearing mean diam.	Ball diameter	Raceway radius	Initial contact angle
541.00 mm	25.00 mm	13.25 mm	45°

Table 1. Nominal dimensions of the measured bearing

2.2. Analytical model for interference calculation

The next step in order to calculate the ball-raceway interferences is to assess the relative position between the inner and the outer ring once the bearing is assembled and the equilibrium is reached. In this regard, the final spatial configuration will be the one with the minimum associated elastic deformation potential energy. Therefore, the key of the proposed method lies on the formulation and the minimization of the energy of the system.

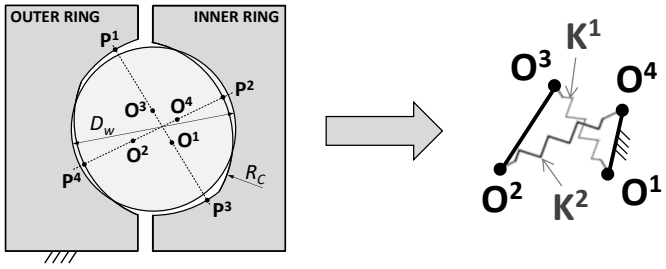

Figure 3. Graphical representation of the mechanism of the analytical model.

For this purpose, the ball-raceway contact model developed and validated by Daidié et al. [15] is used. Taking advantage of this technique, the centres of the raceways from the different rings are linked each other by traction-only springs that simulate the stiffness of the contacts, as shown in Figure 3. Moreover, the centres from the same ring are rigidly connected, assuming rigid rings. This way, each pair of springs represents the four contacts of each ball of the bearing, so the elastic contact problem is simplified by means of the deformable mechanism represented in the figure. For the formulation of the potential energy, the outer ring is fixed, while the position of the inner ring will be a function of the relative displacements and rotations between them. Hence, points O^1 and O^4 of the mechanism are fixed, while the coordinates of points O^2 and O^3 are a function of the parameters X_D, Y_D, Z_D, α and β, represented in Figure 4, which define the position of the inner ring with respect to the outer one.

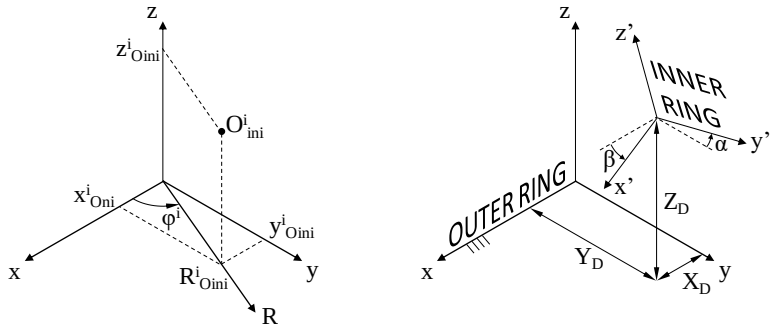

Figure 4. Coordinate systems: (a) cartesian and cylindrical coordinates; (b) parameters for the relative position definition of the inner ring.

As a first step, the coordinates of the centres of the raceways, obtained from the experimental measurements, are changed from the cartesian coordinate system (x, y z) to a cylindrical one (R, φ, z). Following the nomenclature in Figure 4:

$$\begin{aligned} R^i_{Oini} &= \sqrt{\left(x^i_{Oini}\right)^2 + \left(y^i_{Oini}\right)^2} \\ \varphi^i_{Oini} &= atan\left(\frac{y^i_{Oini}}{x^i_{Oini}}\right) \end{aligned} \quad \text{where} \quad i \in [1,4] \tag{1}$$

The outer ring is fixed and thus the position of points O^1 and O^4 remain constant. Conversely, the final coordinates of points O^2 and O^3 will be given by the following expressions in Cartesian coordinates:

$$\begin{aligned} x^i_O &= x^i_{Oini}cos\beta + z^i_{Oini}sin\beta + X_D \\ y^i_O &= y^i_{Oini}cos\alpha - z^i_{Oini}sin\alpha + Y_D \\ z^i_O &= z^i_{Oini}cos\alpha cos\beta - x^i_{Oini}sin\beta + y^i_{Oini}sin\alpha + Z_D \end{aligned} \quad \text{where} \quad i \in [2,3] \tag{2}$$

These expressions are changed into cylindrical coordinates:

$$\begin{aligned} R^i_O &= R^i_{Oini}\left(cos\alpha sin^2\varphi^i_O + cos\beta cos^2\varphi^i_O\right) + \left(X_D + z^i_{Oini}sin\beta\right)cos\varphi^i_O + \left(Y_D - z^i_{Oini}sin\alpha\right)sin\varphi^i_O \\ z^i_O &= z^i_{Oini}cos\alpha cos\beta + R^i_{Oini}\left(sin\alpha sin\varphi^i_O - sin\beta cos\varphi^i_O\right) + Z_D \end{aligned} \tag{3}$$

Note that all the displacements occur in the radial plane, while the angular coordinate (φ) will remain constant:

$$\varphi^i_O = \varphi^i_{Oini} \quad \text{where} \quad i \in [1,4] \tag{4}$$

Since manufacturing errors are being considered, the natural lengths of the springs can be different from each other. For a given circumferential position, and according to the numbering used in Figure 3, the natural length of spring i is given by:

$$l^i_N = R^i_C + R^{i+2}_C - D_w = R^i_C + R^{i+2}_C - (D^{nom}_w + \delta_P) \quad \text{where} \quad i \in [1,2] \tag{5}$$

Where D_w is the diameter of the ball, equal to the nominal diameter D^{nom}_w plus the preload δ_P, and R^i_C the radius of the raceway. On the other hand, the real length (l) will be a function of the position of the inner ring:

$$l^i = \sqrt{\left(R^i_0 + R^{i+2}_0\right)^2 + \left(z^i_0 + z^{i+2}_0\right)^2} \quad \text{where} \quad i \in [1,2] \tag{6}$$

Having both natural and real lengths, the summation of the interferences corresponding to each contact pair linked by each spring will be calculated according to the next expression:

$$\delta^i_{Tot} = \delta^i + \delta^{i+2} = l^i - l^i_N \quad \text{where} \quad i \in [1,2] \tag{7}$$

According to [15], the stiffness of each contact can be expressed as:

$$K^i = \begin{cases} \frac{105283 \cdot D_w^{1/2}}{(1-s^i)^{0.2919}} & \text{if} \quad \delta^i > 0 \\ 0 & \text{if} \quad \delta^i \leq 0 \end{cases} \quad \text{were} \quad i \in [1,4] \tag{8}$$

Where $s^i = D_w/\left(2R_C^i\right)$ is the osculation ratio of the contact i. It is important to point out that, as the springs are traction-only, they do not offer any resistance for the $\delta^i < 0$ case, which represents a gap between the contacting bodies. In the ball-raceway hertzian-type contact, the relationship between the ball normal load (Q) and its deformation (δ) is formulated as:

$$Q = K\delta^{3/2} \tag{9}$$

This formula is valid for elastic deformations with no truncation of the contact ellipse, which is acceptable with the load rates involved in the case under study. From this expression, the total stiffness of the spring i that links the raceway centres i and $(i+2)$ is obtained:

$$\frac{1}{\left(K_{Tot}^i\right)^{2/3}} = \frac{1}{(K^i)^{2/3}} + \frac{1}{(K^{i+2})^{2/3}} \quad \text{were} \quad i \in [1,2] \tag{10}$$

Finally, the potential energy for the entire system formed by B balls will be given by:

$$E_P = \frac{2}{5}\sum_{b=1}^{B}\left[K_{Tot}^{1b}\left(\delta_{Tot}^{1b}\right)^{5/2} + K_{Tot}^{2b}\left(\delta_{Tot}^{2b}\right)^{5/2}\right] \tag{11}$$

Inasmuch as the interferences depend on the five parameters that define the final position of the inner ring, so will the potential energy. The proposed formulation was implemented in Octave and the minimization of the potential energy was performed by means of a gradient based algorithm. No convergence problems were found because potential energy function is continuous and derivable with no local minima; when the function is null (no interferences case), it is not derivable, but that point would directly be the solution. For the particular case studied in the present work, the results for the interferences are shown in Figure 5.

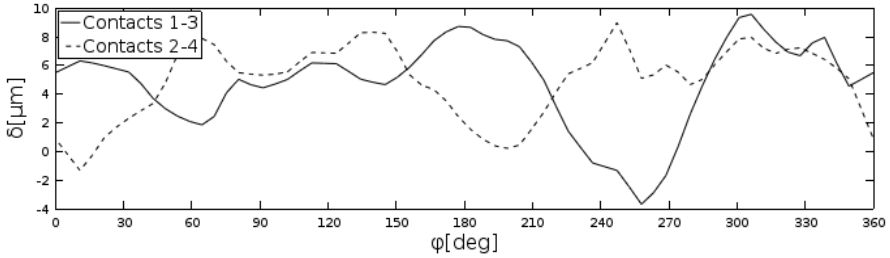

Figure 5. Interferences in the measured bearing with the nominal ball ($D_w = D_w^{nom}$, $\delta_P = 0$).

3. FINITE ELEMENT MODEL FOR FRICTION TORQUE CALCULATION

As it has been mentioned before, the friction torque is a relevant magnitude in slewing bearings. Therefore, it is interesting to evaluate the influence of manufacturing errors in this parameter. With this aim, different FE calculations were performed, whose results are given and compared in the next section.

The FE model is based on the one previously developed by the authors in [10], where only the sector corresponding to one ball is considered. Note that, for the appropriate simulation of the contact behaviour, the contact region was carefully meshed (see Figure 6), with a smooth transition to the coarser surrounding elements. In the contact surfaces, a typical value of 0.1 was taken for the friction coefficient, assuming grease lubrication [8].

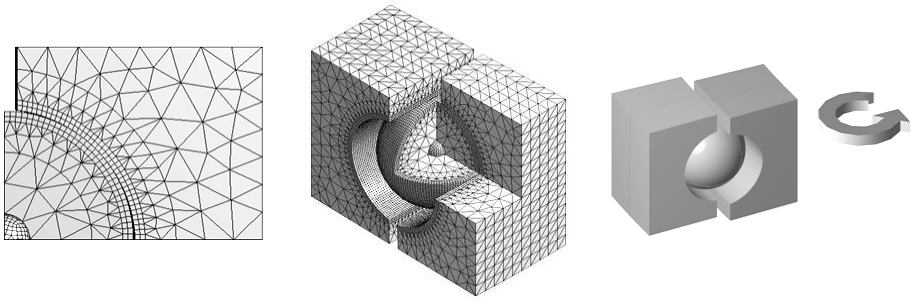

Figure 6. FE model: mesh and applied loads

The ball-raceway interferences, calculated by the analytical model described in the previous section, are introduced in the FE model by imposing an offset to the contacting surfaces of the raceway [12]. Additionally, the model allows introducing a preload by applying a specific thermal condition to the ball in order to oversize it.
Both rigid and deformable rings are considered for the friction torque calculations. In both cases, the elastic behaviour in the contact is suitably simulated, but the difference lies on the boundary conditions and the geometry of the rings. On the one hand, for the case of rigid rings, no deformation is allowed to their external surfaces (thick lines in Figure 7a). Hence, the geometrical parameters D_I, D_O, H, e and ψ (see Figure 8) have a negligible effect in the elastic behaviour of the system, so they are defined only as a function of the diameter of the ball (D_w) according to [10].

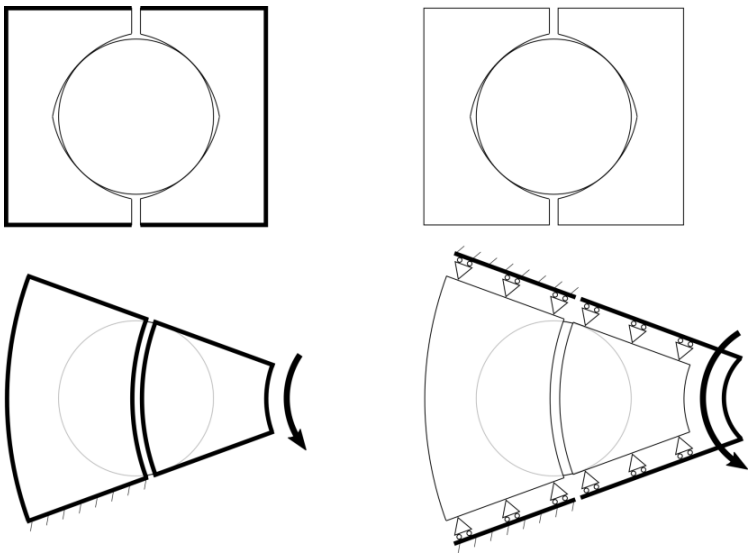

(a) (b)

Figure 7. Boundary conditions of the FE model: (a) rigid rings; (b) deformable rings.

On the other hand, with deformable rings, only the displacements in the normal direction of the lateral faces of the sector are restricted, allowing free sliding movement so that the rings can deform in the radial and axial directions (see figure 7b). Moreover, as the deformation of the system will depend on the deformability of the rings, their real geometry (D_I, D_O, H, e and ψ) must be considered. In addition, it must be pointed out that the sweep angle (ψ) will be a function of the number of balls. Rolling bearings can be mounted with or without spacers, and the dimensions of these ones can be variable, so the number of balls can change, and consequently the value of the sweep angle. As it will be demonstrated, this fact has a relevant effect in the behaviour of the bearing.
The rotation is applied to the inner ring after applying the corresponding interferences and preload, while the outer ring remains fixed. According to Kalker [16], the ball needs to be displaced quasi-statically at least one time an entire contact ellipse in order to achieve the stabilization of the friction torque. Thus, the rotation angle is calculated in such a way that this distance is fully covered.

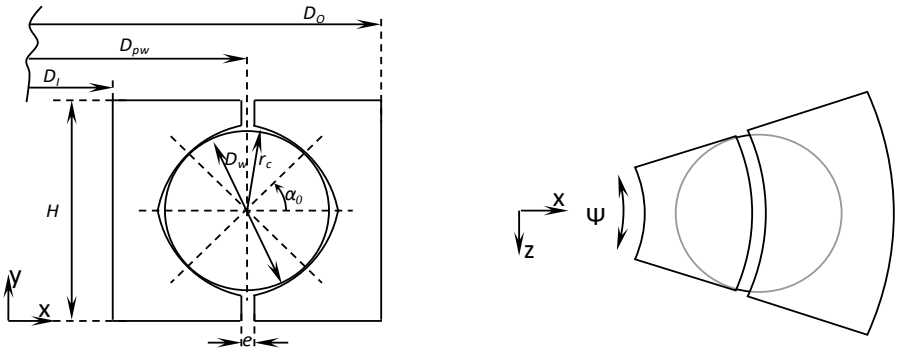

Figure 8. Geometrical parameters of the FE model

As a result, the evolution of the friction torque over time is obtained from the FE model. In order to filter the fluctuations due to the numerical nature of the model and thus obtain a value for the friction torque, the following functional approximation is used [10]:

$$M_f = \frac{M_0(t-1)^\eta}{\beta+(t-1)^\eta} \tag{12}$$

The results for a particular case are shown in Figure 9 together with its corresponding fitting curve. This figure also shows the contact status in a case where the ball is rolling, illustrating the fact that this model considers the stick (in black) and slip (in grey) regions in the contact ellipse.

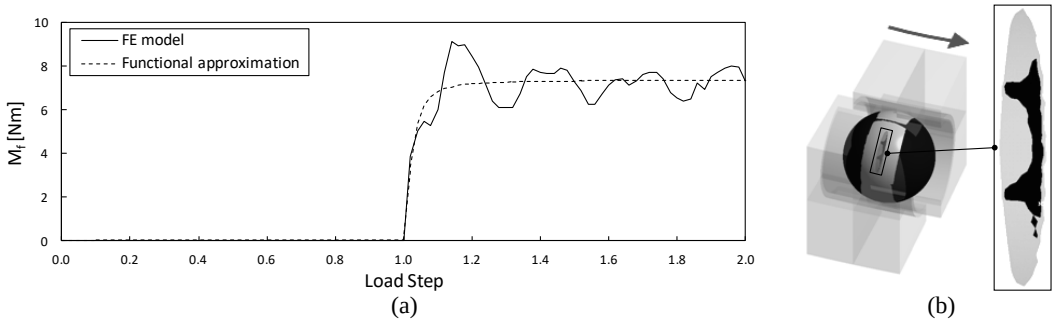

Figure 9. FE results: (a) evolution of the friction torque; (b) contact status.

In order to calculate the friction torque for the whole bearing, as many calculations as balls inside the bearing are needed, introducing for each one its corresponding interferences values. For simplification purposes and to avoid high computational costs, a Design Of Experiments (DOE) was planed considering the 3 parameters related with the tolerances: the interferences in each contact pair (the two interferences δ_1 and δ_2) and the osculation ratio (s). Taking pick and valley values for these parameters, a full factorial DOE was performed considering different levels for the conformity ratio and the interferences. Based on (9) and [15], the next functional approximation is proposed by the authors:

$$M_f = \begin{cases} \frac{C_1(\delta_1^n+\delta_2^n)+C_2(\delta_1+\delta_2)^n}{(1-s)^m} & \text{if} \quad \delta_1 \cdot \delta_2 \neq 0 \\ 0 & \text{if} \quad \delta_1 \cdot \delta_2 = 0 \end{cases} \tag{13}$$

The values for the coefficients are different if the ball is spinning in all contacts or if it is rolling with respect to two points (and thus sliding respect the other two). If contact only exists in two points and the interference is the order of few microns, the friction torque is negligible. In the cases under study, only preload (and no external load) is considered, so there will exist no case with a big interference in one contact diagonal and no contact in the other. To know if a ball is spinning or rolling, the interference ratio (r_δ) is defined, which relates both interferences in each ball:

$$r_\delta = \frac{\max(\delta_1,\delta_2)}{\min(\delta_1,\delta_2)} \tag{14}$$

If this ratio is lower than the transition value (r_δ^{tr}), the ball will be spinning; if not, the ball will be rolling. The values for r_δ^{tr} were determined based on the results from the FE calculations. Table 2 compiles the values for the coefficients from equation (13), which were obtained by the least squares fitting with the points from the DOE. Using the values of Table 2 and introducing δ in [mm] in (13), M_f is obtained in [Nm]. For the model with deformable rings, 32 balls were considered; this aspect is important because the sweep angle (ψ) affects the response of the sector, as previously mentioned.

Rings behaviour	r_δ^{tr}	4 points spinning				2 points rolling + 2 points sliding			
		n	m	C_1	C_2	n	m	C_1	C_2
Rigid	7.5	2.09	0.85	531	28.2	2.09	0.85	-1344	1376
Deformable (32 ball)	3.5	1.81	0.75	291	-84	8.93	1.87	0	3.08E7

Table 2. Values for the functional approximation of the friction torque.

Figure 10 compares the results from the 52 FE calculations of the DOE (markers) with the functional approximation (13) for the case with deformable rings (lines), illustrating the excellent correlation between them (similar correlation appears for the rigid ring case). Several detailed views of two regions of the plot are also shown for clarity. The jump discontinuity in the curves represents the transition related to the kinematic of the ball, from rolling ($r_\delta > r_\delta^{tr}$) to spinning ($r_\delta < r_\delta^{tr}$).

Finally, the proposed formula (13) was used to calculate the friction torque due to each ball, so the total torque can be calculated as the sum of all the balls in the bearing. The results are shown in the next section.

4. RESULTS AND DISCUSSION

The analytical model described in section *2.2* was used to obtain the interference values for the case of nominal ball (Figure 5) and balls with 6 different preloads, ranging from -5μm to +25μm. Feeding (13) with these interference

values, the contribution of each ball to the friction torque for each case was obtained for both rigid and deformable rings (using the coefficients in Table 2).

For the sake of completeness of the work, two additional aspects were considered when calculating the interferences. On the one hand, the relative angular position between the rings, i.e. the rotation of the inner ring in the z axis according to Figure 4. On the other hand, the manufacturing tolerances of the balls (not to be confused with the manufacturing errors of the raceways); the ball quality was grade 40 in this case, which implied a variation of 2μm in the ball diameter from the same lot [17] (this information was provided by balls manufacturer). The results for the total torque of the bearing, with the scatter due to these two factors, are given in Figure 11.

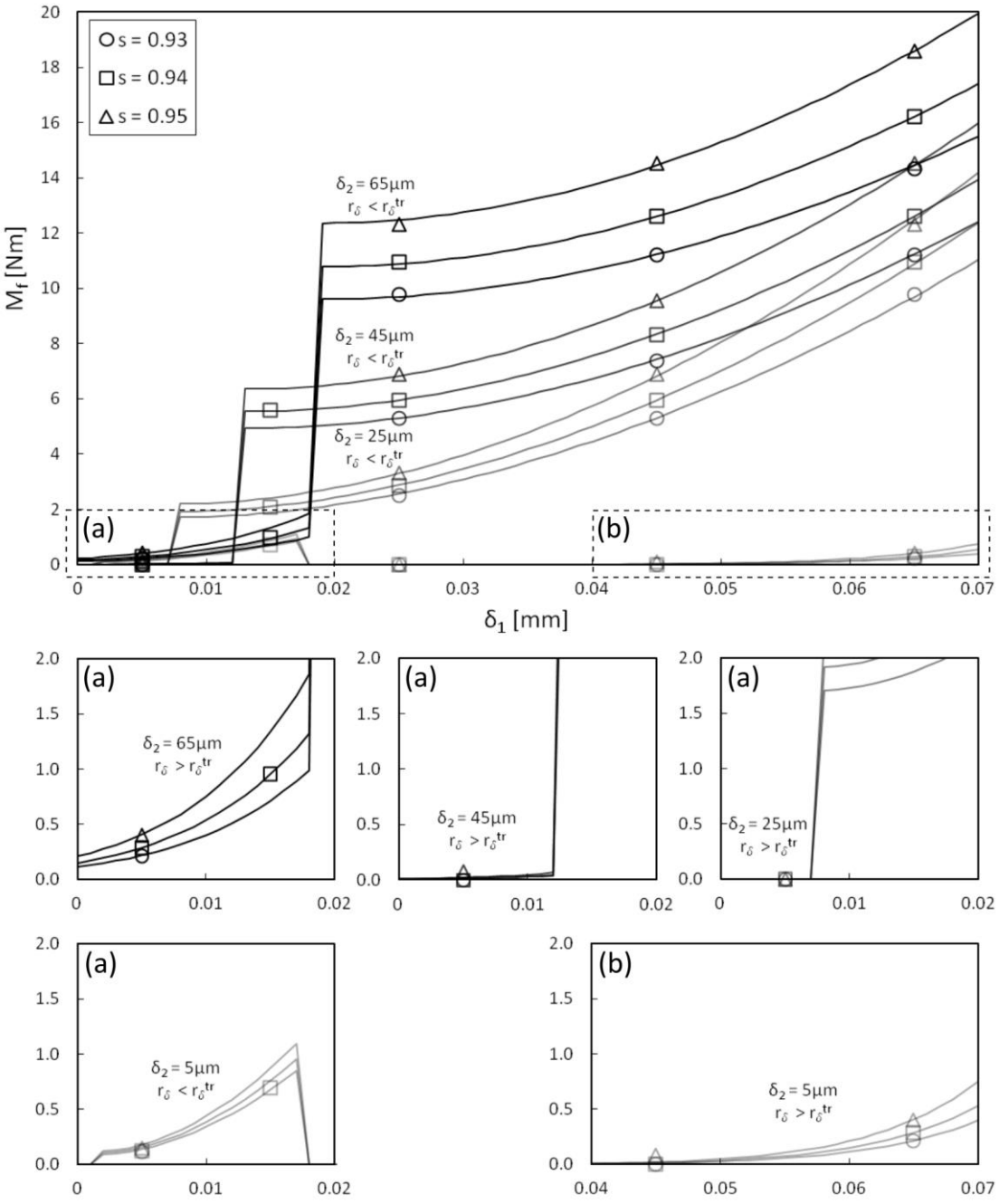

Figure 10. Friction torque results for the DOE (markers) and calculated functional approximation (lines) for deformable rings.

In order to evaluate the effect of manufacturing errors in the friction torque, FE calculations were also performed with the nominal geometry, i.e. with no manufacturing errors, for every preload case; these results are also shown in Figure11. It can be observed that the effect of manufacturing errors have a great influence in the friction torque, ergo they must be considered when accurate results are required. Moreover, the high relevance of the deformability of the rings in the friction torque is also evinced.

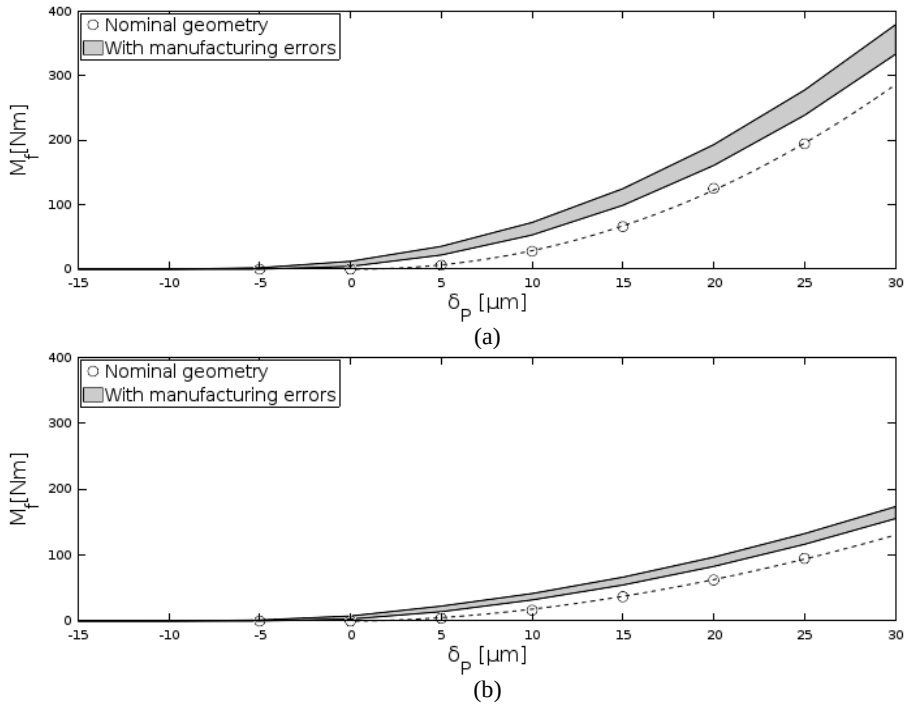

Figure 11. Friction torque VS Ball preload with (band) and without (dotted line) the effect of manufacturing errors: (a) rigid rings; deformable rings

Additionally, the effect of the number of balls in the friction torque was studied. For this purpose, and without taking into account manufacturing errors, FE calculations with deformable rings were performed, varying ball number and preload. It was found that the effect of the number of balls is logarithmical, and the next functional expression proved to properly fit FE results:

$$M_f = C{\delta_P}^n \cdot ln\left(\frac{N}{N_r} + 1\right) \tag{15}$$

Where δ_P is the preload, N is the number of balls and n, C and N_r are coefficients to be determined for each bearing. For this particular case, the values of the coefficients that best fit the FE calculations are 1.84, 0.15 and 8 respectively, so M_f will be obtained in [Nm] if δ_P is introduced in [μm]. Figure 12 shows the results from the FE calculations (markers) and the functional approximation in (15) (solid lines). Furthermore, the results for rigid rings are shown for one preload case (25μm, dotted line), illustrating that if the elasticity of the rings is not considered, the influence of the ball number is linear.

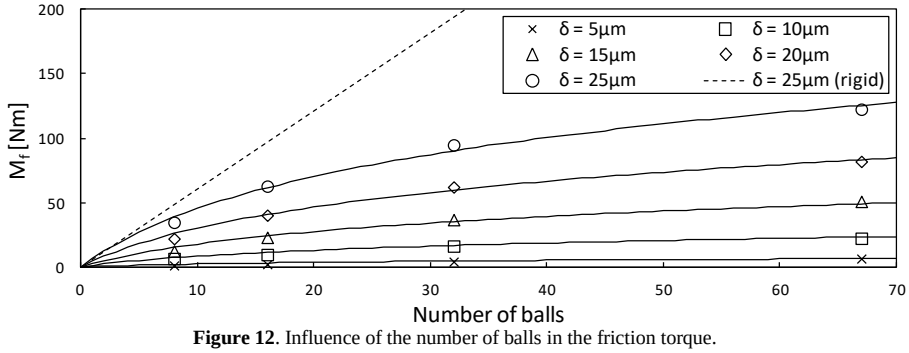

Figure 12. Influence of the number of balls in the friction torque.

5. CONCLUSIONS AND FUTURE WORK

This work presents a procedure for the calculation of the ball-raceway interferences due to manufacturing errors in four contact point slewing bearings. This procedure was applied to a particular case and the values of the interferences were obtained. The results were used to perform Finite Element analyses for the friction torque calculation, which proved that both manufacturing errors and rings deformability have a significant effect in the idling friction torque. Therefore, not considering them will lead to inaccurate results.

Evenly remarkable is the effect the number of balls has in the friction torque, which was found to be logarithmical. A new formula has been proposed and validated via Finite Element calculations, which expresses the friction torque as a function of the number of balls and preload.

Regarding future work, the following research lines have been defined. First, the analytical model for the interferences calculation developed in this manuscript will be generalized to estimate the load distribution among the balls under external load (not only preload). Besides, the stiffness of the rings will also be implemented in the analytical model via superelement techniques by reducing the elasticity of the rings to the centres of the raceways. Thus, in contrast with the state of the art analytical formulations, this model will be able to consider analytically the influence of manufacturing errors and the stiffness of the rings on the assessment of the load distribution in balls. Later, the results of this model will be used as an input data for a second type of analytical model, which will deal with the contact problem in order to calculate the friction torque of the bearing, avoiding the large computational cost of Finite Element Analyses. Finally, some experimental tests will be carried out for correlation purposes.

ACKNOWLEDGEMENTS

This paper is a result of the close collaboration that the authors maintain with the company Iraundi S.A. The authors wish also to acknowledge the financial support of the Ministry of Economy and Competitiveness through project number DPI2013-41091-R, and the University of the Basque Country through project number UFI 11/29.

REFERENCES

[1] S. Zupan, I. Prebil, Carrying angle and carrying capacity of a large single row ball bearing as a function of geometry parameters of the rolling contact and the supporting structure stiffness, Mech. Mach. Theory. 36 (2001) 1087–1103. doi:10.1016/S0094-114X(01)00044-1.

[2] J.I. Amasorrain, X. Sagartzazu, J. Damián, Load distribution in a four contact-point slewing bearing, Mech. Mach. Theory. 38 (2003) 479–496. doi:10.1016/S0094-114X(03)00003-X.

[3] J. Aguirrebeitia, J. Plaza, M. Abasolo, J. Vallejo, General static load-carrying capacity of four-contact-point slewing bearings for wind turbine generator actuation systems, Wind Energy. 16 (2013) 759–774. doi:10.1002/we.1530.

[4] J. Aguirrebeitia, M. Abasolo, R. Avilés, I. Fernández de Bustos, General static load-carrying capacity for the design and selection of four contact point slewing bearings: Finite element calculations and theoretical model validation, Finite Elem. Anal. Des. 55 (2012) 23–30. doi:10.1016/j.finel.2012.02.002.

[5] J. Aguirrebeitia, J. Plaza, M. Abasolo, J. Vallejo, Effect of the preload in the general static load-carrying capacity of four-contact-point slewing bearings for wind turbine generators: theoretical model and finite element calculations, Wind Energy. 17 (2014) 1605–1621. doi:10.1002/we.1656.

[6] A. Leblanc, D. Nelias, Ball Motion and Sliding Friction in a Four-Contact-Point Ball Bearing, J. Tribol. 129 (2007) 801–808. doi:10.1115/1.2768079.

[7] A. Leblanc, D. Nelias, Analysis of Ball Bearings with 2, 3 or 4 Contact Points, Tribol. Trans. 51 (2008) 372–380. doi:10.1080/10402000801888887.

[8] A. Joshi, B. Kachhia, H. Kikkari, M. Sridhar, D. Nelias, Running Torque of Slow Speed Two-Point and Four-Point Contact Bearings, Lubricants. 3 (2015) 181–196. doi:10.3390/lubricants3020181.

[9] A.B. Jones, Ball Motion and Sliding Friction in Ball Bearings, J. Basic Eng. 81 (1959) 1–12.

[10] J. Aguirrebeitia, M. Abasolo, J. Plaza, I. Heras, FEM model for friction moment calculations in ball-raceway contacts for applications in four contact point slewing bearings, in: 14th World Congr. Mech. Mach. Sci. 25-30 Oct., Taipei, Taiwan, 2015.

[11] S. Kang, D. Tesar, An analytical comparison between ball and crossed roller bearings for utilization in actuator modules for precision modular robots, in: ASME 2003 Des. Eng. Tech. Conf. Comput. Inf. Eng. Conf. Sept. 2-6, Chicago, Illinois, USA, 2003: pp. 1221–1230. doi:10.1115/DETC2003/DAC-48834.

[12] S. Aithal, N. Siva Prasad, M. Shunmugam, P. Chellapandi, Effect of manufacturing errors on load distribution in large diameter slewing bearings of fast breeder reactor rotatable plugs, Proc. Inst. Mech. Eng. Part C J. Mech. Eng. Sci. 0 (2015) 1–12. doi:10.1177/0954406215579947.

[13] M. Olave, X. Sagartzazu, J. Damian, A. Serna, Design of Four Contact-Point Slewing Bearing With a New Load Distribution Procedure to Account for Structural Stiffness, J. Mech. Des. 132 (2010) 21006. doi:10.1115/1.4000834.

[14] I. Heras, J. Aguirrebeitia, M. Abasolo, Calculation of the Ball Raceway Interferences Due to Manufacturing Errors and Their Influence on the Friction Moment in Four-Contact-Point Slewing Bearings, in: P. Wenger, P. Flores (Eds.), New Trends Mech. Mach. Sci. Theory Ind. Appl., Springer International Publishing, Cham, 2017: pp. 3–11. doi:10.1007/978-3-319-44156-6_1.

[15] A. Daidié, Z. Chaib, A. Ghosn, 3D Simplified Finite Elements Analysis of Load and Contact Angle in a Slewing Ball Bearing, J. Mech. Des. 130 (2008) 82601. doi:10.1115/1.2918915.

[16] J.J. Kalker, Three-Dimensional Elastic Bodies in Rolling Contac, Springer Netherlands, 1990. doi:10.1007/978-94-015-7889-9.

[17] ISO 3290-1:2014, Rolling bearings - Balls - Steel balls, 2014.